ECCOMAS Congress 2016
VII European Congress on Computational Methods in Applied Sciences and Engineering
M. Papadrakakis, V. Papadopoulos, G. Stefanou, V. Plevris (eds.)
Crete Island, Greece, 5–10 June 2016

EXPLICIT DARCY'S LAW BOUNDARY CONDITION WITH COMBINED CONTINUUM AND DISCRETE MODEL FOR PRESSURE DRIVEN MEMBRANE APPLICATIONS

Tomi I. Naukkarinen[1], **and Teemu Turunen-Saaresti**[1]

[1] School of Energy Systems, Lappeenranta University of Technology (LUT)
Skinnarilankatu 34,53850 Lappeenranta, Finland
e-mail: tomi.naukkarinen, teemu.turunen-saaresti@lut.fi

Keywords: CFD-DEM, Darcy's law, Membranes, Dilute solute.

Abstract. *In this paper Darcy's law for dilute solutes, that is implemented explicitly to a boundary condition in computational fluid dynamics-discrete element method (CFD-DEM) solver, is presented for pressure driven membrane applications. The explicit treatment of the boundary condition with Darcy's law in segregated pressure based solver induces oscillations. To avoid oscillations the boundary condition is under relaxed by limiting change of the solvent flux between iteration cycles. With combination Darcy's law and CFD-DEM cake formation on a membrane and some of the hybrid processes can be modeled.*

1 INTRODUCTION

Pressure driven membrane process is widely used in civil engineering (e.g municipal wastewater and the desalination of sea water or brackish) and industry. The pressure driven processes suffer of fouling like other membrane processes. The fouling is a severe problem which increases maintenance cost, decreases productivity and in the some cases forces to shut down process. Cake formation, one type of the fouling, can be the problem at the membrane where it directly increases flow resistant, or at pretreatment phase, where solids are removed. In the former case, a cake effects indirectly to energy consumption and increases required pumping power.

Water quality regulations and the concern of trace contaminants imposes requirements to a water treatment technology and raises new ways to treat water e.g. hybrid ion exchange (IE) - pressure driven membrane processes as Al Abdulgader et al. [1] pointed out. In many hybrid IE-pressure driven membrane processes ion exchange and filtration is separated to different units while Kabay et al. [2] suggested hybrid process where ion exchange resins were immersed in feed and retentive. According Kabay et al. [2] in submerged system yield and separation efficiency is at high level. The submerged systems could be alternative method to traditional fixed bed columns.

Cake formation on a membrane and submerged hybrid processes impose additional requirements to modeling, particularly for computational fluid dynamics (CFD). Particle-particle collision and fluid-particle interaction forces have to be considered while flow regime changes from dilute to dense [3]. In addition, at small particle ($\sim \mu$m) scales cohesion forces have important role in settling and filtration [4]. Dong et al. [4] modeled successfully settling and filtration with DEM code but they assumed direction of fluid flow and used periodic boundary conditions. To gather information from systems, larger scale modelling e.g. fluidization or pneumatic convey is required [5].

Modeling of pressure driven membranes with CFD are common divided in two approached based on a boundary condition used for a membrane; dissolving and permeating boundary conditions [6]. Both of those approaches assumes boundary layer on membrane at permeate stream can be neglected which means constant pressure and concentration at the permeate stream. In addition, a membrane is modeled as boundary condition. In dissolving method there is no flux through a membrane and solute's boundary condition type is either is Dirichlet or Neumann. Use of the dissolving boundary condition can be justified by small modeling area where Reynolds number does not change. In the permeating boundary condition the solvent flux is defined by a equation similar to Darcy's law which is depend on the transmembrane pressure (TMP) and osmotic pressure [7]. Transmembrane pressure is pressure difference between feed and permeate streams. The pressure difference is the potential and the driving force for separation in the pressure driven membrane separation. The driving pressure is decreased by osmotic pressure. Osmotic pressure is pressure which is needed to prevent solvent flux across a semipermeate membrane from dilute solution to concentrate solution. Osmotic pressure rises from osmosis phenomenon. Osmotic pressure is proportional to solute concentration differences and solute type.

Drag, which is depended on the relative velocity difference and which is the one of the major

forces in the particle-fluid flows, has large impact on the pressure loss in the cake or resin bead layer. The drag force transfer momentum from the fluid to the particles and vise versa depend on the relative velocity difference. However, the pressure loss decreases TMP which decreases relative velocity difference and this interconnection effect is only possible to model with permeating boundary condition. Results of Dong et al. [4] support this assumption.

In this paper, Lagrangian-Euler approach, which is implemented to CFD-DEM program [8], is used with the explicit Darcy alike equation [6] to model particle fluid flow with the permeating membrane. The osmotic pressure is not included and only hydrodynamic model is taken account at this point. In addition, the segregated pressure-velocity coupling and PISO-loop [9] is used.

2 Numerical Methods and Case Setup

Permeating flux through the membrane is sensitive to TMP, which is solution of the pressure-velocity field, and at the same time the flux effects to velocity and pressure fields. This dependence with updating boundary values at the end of PISO-loop raise problems to achieve convergent solution.

To solve the convergence problem relaxation is added to the membrane boundary condition:

$$\begin{cases} \mathbf{J_{slv}} = \alpha \mathbf{J^o_{slv}} + (1-\alpha) L_p \Delta p_{tm} \hat{\mathbf{n}}, & \text{if } \|\mathbf{J_{slv}} - \mathbf{J^o_{slv}}\| \leq \beta \\ \mathbf{J_{slv}} = \mathbf{J^o_{slv}} + \beta \dfrac{\Delta p_{tm}}{\|\Delta p_{tm}\|} \hat{\mathbf{n}}, & \text{if } \|\mathbf{J_{slv}} - \mathbf{J^o_{slv}}\| > \beta \end{cases} \tag{1}$$

where $\mathbf{J_{slv}}$ is solvent flux, L_p is hydraulic permeable coefficient, Δp_{tm} is transmembrane pressure and superscript 0 is the mark of previous iteration. $\hat{\mathbf{n}}$ is surface normal. The equation 1 is sensitive to three parameters: α, β and L_p. Hydraulic permeable coefficient L_p is the most important factor since it defines membrane sensitivity of TMP. α has relaxing effect to equation 1 and effects directly convergence rate. β prevents diverging changes of flux between iteration rounds.

Within this paper pseudo-2D test computational domain is used: the flow is modeled in 2D and the particles are calculated with the 3D slice. The slice is used similar way in Ketterhagen et. al [10] to reduce computational demand and to take into account the three dimensional effects of particles. The computational domain is shown in figure 1. The flow with particles is introduced from the left, between the backward- and forward-facing step lies the membrane, where solvent permeates, and some of the particles are settled on the membrane. Rejection with some particles flows out of the domain at the right. A list of dimensions of test domain is shown in table 1. All test cases start with fully developed flow field without any particles. Solid mass fraction is fixed to 0.25 at the inlet until 300k of particles are fed in the flow domain. Constant and uniform velocity is used (0.5 m/s) at the inlet. Outlet pressure is set to be 109000 Pa. Constant viscosity is also assumed. Twenty pressure-velocity corrections per a time step are used to achieve convergent solution as a compromise between computational demand and accuracy.

In the test cases, boundary condition's ability to respond changing flow circumstances and the sensitivity of parameters α and β are tested. In the first case the variety of α values and the fixed β value are used. Table 2 includes the variables values of case I. In the case II limiter

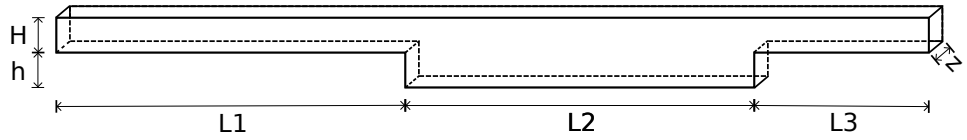

Figure 1: Outlay of computational domain

Property	value	Unit
Geometry		
H	0.01	m
h	0.01	m
L1	0.1	m
L2	0.1	m
L3	0.05	m
z	0.001	m

Table 1: Dimensions of the test cases

parameter β is tested by increasing TMP by 50 kPa during one fluid time step (0.000025 s). Three α values are chosen with six different β values as can be seen from table 3. In the third case the sensitivity of relaxation factor α to the hydraulic permeable coefficient L_p, which is multiplied by γ compared to the previous cases, is tested. Table 3 points out γ values.

3 Results and Discussion

Averaged modeled solvent flux through the membrane is compared to the averaged result of equation 2. Basically the equation 2 is the same as the equation 1 without relaxation and the results of equation 2 are calculated with the modeled pressure on the membrane. Comparison is done by using absolute and relative errors. In the case I the averaged fluxes are calculated at time 0.3 s which is about 0.05 seconds after particles hit membrane surface and induces pressure fluctuations. The flow field and the particle distribution are illustrated in figure 2 and the error results of the cases I are presented in table 4. α value 0.99 produces good results in the case I since the relative and absolute errors are minimal. α value 0.98 or lower produces over 50% relative errors, in addition absolute error that indicates that the flow direction is inward at the membrane. The case I results highlight sensitivity of the explicit boundary condition since only α value 0.99 produce reasonable results. These results indicates that strong relaxation is needed if pressure over membrane changes significantly, e.g filtration changes to backflush.

$$J_{slv,ave} = L_p \Delta p_{tm,m} \tag{2}$$

Case I	α[-]	β[-]	$L_p[m/(sPa)]$
A	0.99	0.005	2.77e-9
B	0.98	0.005	2.77e-9
C	0.97	0.005	2.77e-9

Table 2: Parameters of relaxation factors in case I

	Case II					Case III		
	1	2	3					
	α[-]	α[-]	α[-]	β[-]	$L_p[m/(sPa)]$	α[-]	β[-]	γ[-]
A	0.99	0.9875	0.985	10^{-6}	2.77e-9	0.99	0.005	0.8
B	0.99	0.9875	0.985	10^{-5}	2.77e-9	0.99	0.005	0.9
C	0.99	0.9875	0.985	10^{-4}	2.77e-9	0.99	0.005	1.0
D	0.99	0.9875	0.985	10^{-3}	2.77e-9	0.99	0.005	1.1
E	0.99	0.9875	0.985	10^{-2}	2.77e-9	0.99	0.005	1.2
F	0.99	0.9875	0.985	10^{-1}	2.77e-9	0.99	0.005	1.3
G	0.99	0.9875	0.985	10^{-0}	2.77e-9	0.99	0.005	1.4

Table 3: Parameters in the case II and III

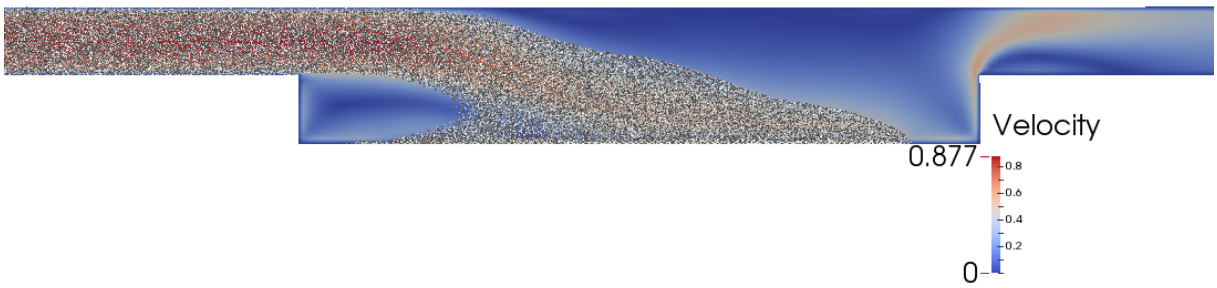

Figure 2: Particle distribution and flow field at 0.3 s in the case I

The error results of case II suggest that large β values are neglecting the limiting part of function in the equation 1 which leads to oscillations, on the other hand small β value slows convergence. In addition, if large enough α value is chosen only small β value can be disadvantage. The relative and absolute error results of the case II are gathered at the next time step after TMP changes and presented in table 5. In the case II the small values ($10^{-6} - 10^{-5}$) of β slows convergence and errors stay at around 80 $\%$. In the caseII(1) α value 0.99 is not sensitive to bigger ($> 10^{-5}$) β values so relative error stays at around 1 $\%$. In the case II(2) errors are first reducing while β value increases, the minimum errors occurs when β is 10^{-3}. After reaching minimum relative error it is increasing again and 10 $\%$ relative error occurs when β reaches value 1. If too small α value is chosen, as in the case II(3), the limiter prevents divergence but solution oscillates inside limiters boundaries.

	Case I	
	rel.[%]	abs. [m/s]
A	0	0.0000
B	92	0.2795
C	179	-0.4006

Table 4: Relative and absolute errors in the case I

	Case II						Case III	
	1		2		3			
	rel.[%]	abs. [m/s]	rel.[%]	abs. [m/s]	rel.[%]	abs. [m/s]	rel.[%]	abs. [m/s]
A	84	0.1360	84	0.1362	84	0.1359	0	0.0000
B	81	0.1120	81	0.1120	81	0.1116	0	0.0000
C	1	0.0003	1	0.0003	677	-0.0236	0	0.0000
D	1	0.0001	0	0.0001	70	0.0636	0	0.0000
E	1	0.0001	1	0.0003	94	0.5560	0	0.0000
F	1	0.0001	1	0.0003	100	-6.5918	1	-0.0012
G	1	0.0001	10	-0.0025	98	72.6242	319	-0.1068

Table 5: Relative and absolute errors in the case II and III

The results, which can be found from table 5, of the case III clarify that there is dependency between L_p and relaxation factor α. Decreasing γ value does not effect to errors but increasing γ value increases both relative and absolute errors and induces oscillations. When γ value exceed 1.3 the errors increase fast. This result suggest that there is minimum α value for every L_p value which can still produce convergent solution. In the other words higher relaxation is demanded if L_p increases.

The presented boundary condition is able to follow the pressure drop of packed particles as can be seen from figure 3. In the figure 3 the case I(A)'s averaged modeled flux and results of equation 2 are presented from 0 s to 2 s. Between fluxes there are good agreement over hole sample time. In the beginning of the simulation flux is constant until particles start packing on the membrane. Packing particles induces pressure loss resulting in flux decreases until particles are fed in the domain and the hight of bed saturates.

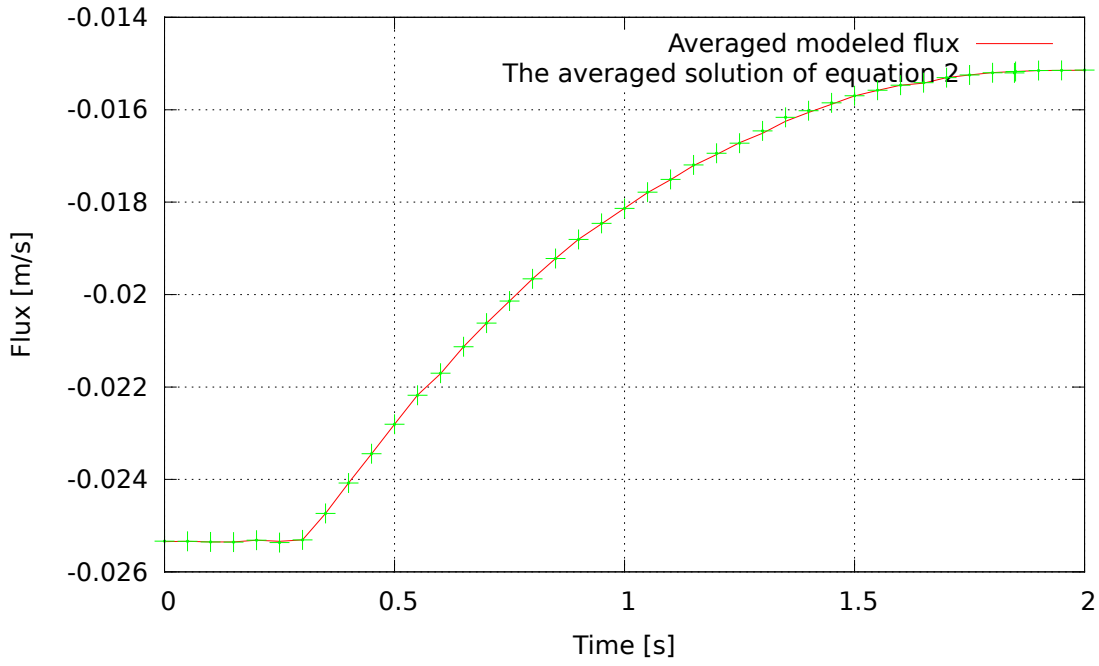

Figure 3: Averaged modeled flux and averaged flux of equation 2 over time in the case I(A)

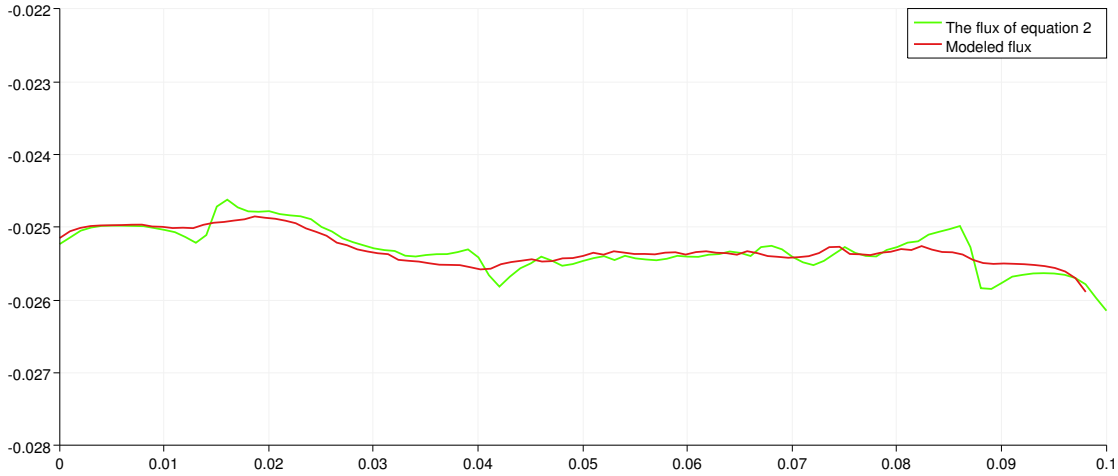

Figure 4: Flux of equation 2 and modeled flux through the membrane at 0.3 s in the case I(A)

The averaged results of equation 2 and the averaged modeled fluxes are almost equal but point-to-point values on the membrane differ. This is revealed in the figure 4 where non-averaged fluxes of the Case I(A) are plotted at 0.3 s. In the figure 4 fluxes are mainly at good agreement but at 0.015, 0.04 and 0.09 m fluxes differ. The spots (0.015 and 0.09 m) where modeled flux lags behind are the same spots where packed bed end in the figure 2. The lag proposes that more pressure-velocity corrections i.e inner iterations are needed and average agreement does not correlate with local unity.

The Darcy alike boundary condition has effect to particle distribution on the membrane as can be seen from figure 5. In the figure 5 the case I(A) is compared to constant flux case at 2 s. The constant flux is same as in the beginning of the case I(A) (-0.0254 m/s). The case I(A) is the upper picture in the figure 5 and the constant flux is lower picture in the figure 5. There are more particles in the constant flux case but in the case I(A) particles are more even distributed after the forward-facing step.

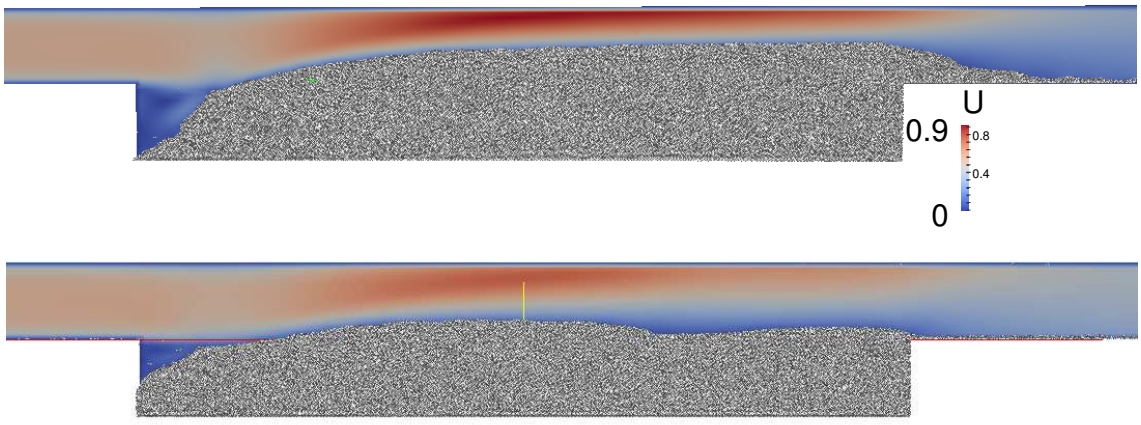

Figure 5: The flow field and particle distribution at 2 s in the constant flux set up (upper) and in the case I(A) (lower).

4 CONCLUSIONS

In this paper explicit Darcy alike equation with relaxation factor and limiter was implemented to model permeate boundary condition. From the results can be seen the boundary condition is able to follow changing flow conditions. However, relaxation is needed and demand of relaxation depend on hydraulic permeable coefficient L_p and pressure changes on a membrane. The used limiter can prevent divergence but small limiter value does not assure convergence which is why it can not be used alone.

REFERENCES

[1] H. Al Abdulgader, N. Hilal, Hybrid ion exchange - pressure driven membrane processes in water treatment: A review. *Separation and Purification Technology*, **192**, 253–264, 2013.

[2] N. Kabay, I. Yilmaz, M. Bryjak, M. Yuksel, Removal of boron from aqueous solution by a hybrid ion exchange-membrane process. *Desalination*, **198**, 158–165, 2006.

[3] H.P. Zhu, Z.Y. Zhou, R.Y. Yang, A.B. Yu, Discrete particle simulation of particulate systems: Theoretical developments. *Chemical Engineering Science*, **62**, 3378–3396, 2007.

[4] K.J. Dong, R.P. Zou, A.B. Yu, G. Roach, DEM simulation of cake formation in sedimentation and filtration. *Minerals Engineering*, **22**, 921–930, 2009.

[5] H.P. Zhu, Z.Y. Zhou, R.Y. Yang, A.B. Yu, Discrete particle simulation of particulate systems: A review of major applications and findings. *Chemical Engineering Science*, **63**, 5728–5770, 2008.

[6] G.A. Fimbres-Weihs, D.E. Wiley, Review of 3D CFD modeling of flow and mass transfer in narrow spacer-filled channels in membranes modules. *Chemical Engineering and Processing*, **49**, 759–781, 2010.

[7] U. Merten, Flow relationships in reverse osmosis. *Industrial & Engineering Chemistry Fundamentals*, **2**, 229–232, 1963.

[8] C. Goniva, C. Kloss, N.G. Deen, J.A.M. Kuipers, S. Pirker, Influence of rolling friction on single spout fluidized bed simulation. *Particuology*, **10**, 582–591, 2012.

[9] R.I Issa, Solution of the implicitly discretised fluid flow equations by operator-splitting. *Journal of Computational Physics*, **62**, 40–65, 1986.

[10] W.R. Ketterhagen, Modeling granular segregation in flow from quasi-three-dimensional, wedge-shaped hoppers. *Powder Technology*, **179**, 126–143, 2008.